Micromachined SU-8-based terahertz 8×8 slotted waveguide antenna array

Mahmud, Rashad H.; Salih, Idris H.; Awl, Halgurd N.; Shang, Xiaobang; Wang, Yi; Skaik, Talal; Lancaster, Michael J.

DOI:
10.1007/s10762-021-00830-6

Micromachined SU-8 Based Terahertz 8×8 Slotted waveguide Antenna Array

Rashad H. Mahmud[1,2*], Idris H. Salih[3], Halgurd N. Awl[4], Xiaobang Shang[5], Yi Wang[2], Talal Skaik[2], and Michael J. Lancaster [2]

[1] School of Electronics, Electrical and Systems Engineering, University of Birmingham, Birmingham B152TT, U.K;
[2] Physics Department, Salahaddin University-Erbil, Iraq, 44002; rhm11286@yahoo.co.uk
[3] Mechatronic Engineering, Faculty of Engineering, Tishk International University, Erbil 44001, Iraq.
[4] Department of Communication Engineering, Sulimani polytechnic University, Sulaimani, 46001, Iraq.
[5] National Physical Laboratory (NPL), UK.
* Correspondence

Rashad H. Mahmud, School of Electronic, Electrical, and Systems Engineering, University of Birmingham, Birmingham, UK.

Email: rhm11286@yahoo.co.uk

Abstract: This article presents the design and fabrication of a micromachined 300 GHz planar array slotted waveguide antenna utilising the silver-coated SU-8 photoresist layer technology. The array is configured to be built from five SU-8 layers of equal thicknesses. The top layer is devoted to form the 8×8 slots. The following three layers are to form the feed and radiating waveguides. The bottom layer is to enclose the design and allocate the input port. An H-plane waveguide bend based on the matching steps is designed and integrated with the proposed array. This is to maintain a precise alignment with the standard waveguide flange WR-03 and facilitate the measurement. Also, two brass-pates are used to clamp the five layers together and tight them via screws in order to minimise the losses. The simulated antenna realised gain is 24.59 dBi, and the 3-dB gain bandwidth is 4.5 GHz. The radiation patterns are very directive, having low side lobe levels. The reflection coefficient has been measured and presented. The proposed micromachined antenna array is directional and low-profile, and may find applications in indoor wireless applications and sensors.

Keywords: Micromachined Technology; SU-8 layers; terahertz antennas; waveguide antennas; slot arrays; micromachining; waveguide bends; SU-8 layers

Acknowledgments: The authors would like to thank the EDT research group at the University of Birmingham, UK, and the Rutherford Appleton Laboratory, Dicot, UK for fabricating and measuring the device.

---

1. Introduction

The terahertz (THz) electromagnetic waves have received significant attentions more recently not only in the detection and imaging systems [1-3], but also in biology and surveillances [4-6]. This is due to increasing the data rate capability of the communication systems and providing a larger bandwidth [5]. Also, THz waves have a better penetration of materials in comparison with the infrared [7]. This is extremely useful in the surveillance applications to scan and extract information from the luggage without opening it. However, this is applicable only for a short-range distance due to the THz atmospheric path loss [8]. To overcome this, employing a high gain antenna at the THz communication system is considered as one of the ultimate solutions.

Many THz communication systems employ optical antennas including lenses and reflectors due their fabrication simplicity, and achieving high gain by increasing their electrical sizes [9, 10]. However, packaging these kinds of antennas with the whole THz systems is difficult due to their curvature shape. Horn antennas, which are high gain and very efficient antennas, are also good candidates for THz systems. The flared out shape of the horns and their dramatic size reduction when operating at THz frequencies, which are expensive and difficult to fabricate, make them less desirable [11]. The planar antennas are good candidates to employ at THz systems due to the fact that they integrate with other THz components easily. Also, they are suitable to be fabricated using the micromachining SU-8 multilayer technology which is considered to be one of the most cost-effective techniques [11-15]. Metal-graphene and Metal-assisted chemical etching structures have also been utilized recently in the design of planar components at the THz spectrum [16-18].

Despite their compactness and good radiation performances, microstrip patch antennas are less desirable applicants to THz systems due to the significant losses [19, 20]. More recently, investigations on achieving high gain and large bandwidth of the periodic reflective surfaces (PRSs) have been conducted at millimeter-wave [21-23] and lower THz frequency bands [24]. Slotted waveguide antennas are high gain antennas which are attractive to THz applications due to their planar structure, low losses, and handling high powers [25-31]. In addition to that, slotted waveguide antennas have structures which are very compatible with the micromachining fabrication Technology [11-13, 32].

In this paper, we design and fabricate a 300 GHz planar array 8×8 slotted waveguide antenna based on the micromachined SU-8 technology which is available at the University of Birmingham. The array is configured to be built from five SU-8 silver-coated layers. An H-plane bend is designed and embedded with the array in order to facilitate the measurements with the standard waveguide flange WR-03. Fabrication has been made, and the reflection coefficient has been measured. More details follow.

2. Antenna Design and Configuration

This section describes the design of the planar array 8×8 slotted waveguide antenna operating at centre frequency f_0= 300 GHz as shown in Fig 1. For clarifications, the outstanding structure in Fig. 1 in the central area shows the hollow radiating waveguides, feeding waveguide, and radiating slots. While the surrounding conductors are set to be transparent.

There are several possibilities to cut the slots in the walls of the rectangular waveguides [33], depending on the desire of the applications [34-36]. In this work, the slots at the centre of the narrow wall of the waveguides are chosen. Because they are more compatible with the micromachined technology [11], which will be utilized in the fabrication of the array as will be discussed later.

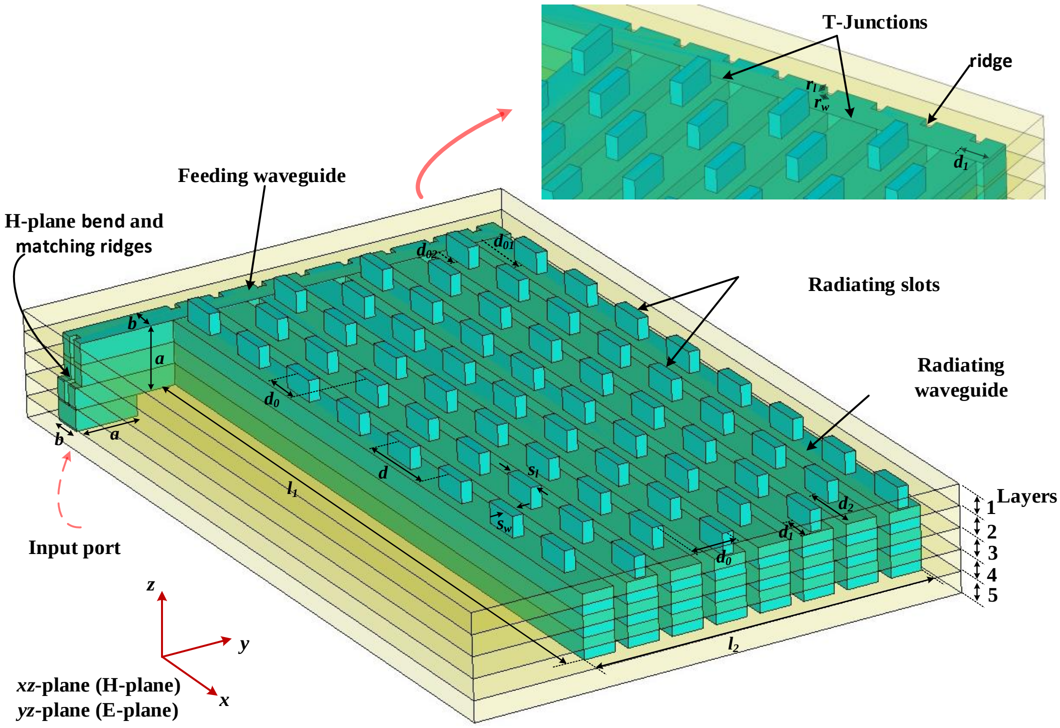

Figure 1. The 3D configuration of the 8×8 narrow-wall slotted waveguide antenna.

The slot length (S_l) and width (S_W) are determined following the fundamental assumptions of slots on the walls of rectangular waveguide [34], as follows;

$$2\log\left(\frac{\text{Slot length }(S_l)}{\text{Slot width }(S_W)}\right) \gg 1 \tag{1}$$

The S_l and S_w dimensions are functions to the operating free space wavelength (λ_0). Where; $\lambda_0 = c/f_0$, and c is the speed of the propagation of electromagnetic wave in free space. In order to excite the slots and obtain good radiations, the S_l needs to be close to $S_l = 0.464\,\lambda_0$, while the $S_w = 0.05\lambda_0$ [37]. In this work, these two relationships are taken into account during the design of the proposed 8×8 slots at f_0=300 GHz. Later, the CST genetic algorithm optimisation [38] method is used in order to optimize these two slot dimensions and enhance the reflection coefficient (S_{11}) at 300 GHz. Another parameter, which also needs to be taken into account in the design, is the inter spacing (d) between the slots. The slots here are placed one-guided wavelength ($d = 1\lambda_g$) a part between the centers as shown in Fig. 1. This is to excite all the slots in-phase. λ_g inside the rectangular waveguides is always greater than free space wavelength (λ_0). It can be calculated, for the dominant mode (TE_{10}), as follows [39];

$$\lambda_g = \frac{\lambda_0}{\sqrt{1-\left(\frac{\lambda_0}{2a}\right)^2}} \tag{2}$$

Where a is the broad-wall dimension of the waveguide.

According to the antenna array theory principle, the $1\lambda_g$ is extremely large. It degrades the radiation patterns and yields grating lobes [40]. This has been experienced practically in our previous work [11, 15, 25, 32, 41]. To overcome this issue, the slots on a radiating waveguide are altered by d_0 ($d_0 = 0.5\lambda_g$) with the neighbour slots as can be noticed in Fig. 1. By means of this alteration, the d value is reduced in the *x-y* planes and the grating lobes disappear as will be depicted later. There are 8 radiating waveguides attached to the feeding waveguide, forming 8 T-junctions as highlighted in the enlargement section of Fig. 1. Ridges are introduced at each of the T-junctions to achieve matching. The radiating waveguides are short-circuited. This is to yield the same phase between the reflected and incident waves.

In order to facilitate the measurements, a waveguide bend is integrated with the proposed antenna array. It is seen in Fig. 2 (a) that the bend has three matching ridges in order to be compatible with the configuration of the array. Also, the matching ridges dimensions (m_1, m_2, w_1, w_2) are optimised so as to obtain a reflection coefficient (S_{11}) from the bend that has negligible impact on the S_{11} response of the antenna array. The optimised S_{11} response of the bend is presented in Fig. 2 (b). It can be depicted that the S_{11} is below -20 dB between 260-315 GHz. The physical dimensions of the proposed antenna array and the H-plane bend are summarized in Table 1.

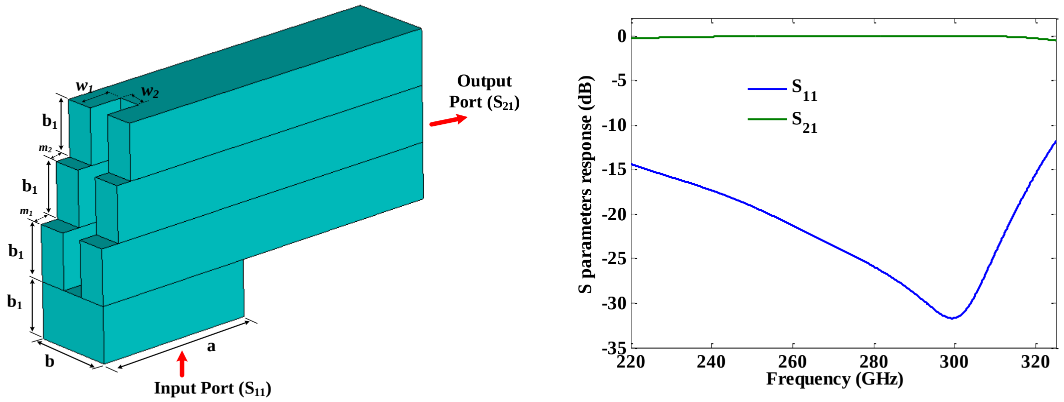

(a) (b)

Figure 2. The H-plane bend embedded to the planar array. (a) the 3D layout of the bend. (b) the solely simulated response of the bend obtained from CST.

Table 1. Dimensions of the proposed THz 8×8 planar array slotted waveguide antenna.

Physical Descriptions	**Symbols**	**Dimensions in mm**
Waveguide cross-section	$a \times b$	0.864 × 0.432
Inter-spacing distance	d	1.226
Radiation Area	$l_1 \times l_2$	9.903 × 4.723
Slots size	$S_l \times S_w$	0.578 × 0.134
Neighbour slot offset	d_0	0.613
Irises dimension	$r_l \times r_w$	0.131 × 0.123
SU-8 layer thickness	b_1	0.288
Last slots terminations	$d_1 \times d_2$	0.307 × 0.920
First slots-feeding waveguides	$d_{01} \times d_{02}$	1.014 × 0.401
Matching ridges	$w_1 \times w_2$	0.187 × 0.139
Matching steps	$m_1 \times m_2$	0.1 × 0.9

The proposed planar antenna array is simulated using the CST simulator [38] as shown in Fig. 3. The Silver material is chosen in CST to build the antenna because the SU-8 layers is planned to be coated by sliver after the fabrications as discussed in Section 3. The simulated S_{11}, realised gain, and directivity variations versus the operating frequencies are shown in Fig. 4. It can be seen that there is a very good matching of S_{11} at f_0 = 300 GHz. Also, the fractional bandwidth (FBW) is ~1 % at S_{11}= -10 dB. The peak directivity and realised gain are 25.2 dBi and 24.6 dBi, and they are very close to each other particularly at f_0 = 300 GHz. This indicates that the antenna is efficient as can be noticed in Fig. 5. The 3-dB gain bandwidth is 4.5 GHz. The radiation patterns for both the E- and H-planes are shown in Fig. 6. They are extremely directive and the main beam is stable from 298-302 GHz. The side lobe levels are very low especially in the E-plane, which is less than -22 dB below the main beam. This is due to having large radiating area in that plane. The performance of the proposed antenna array is summarized in Table 2.

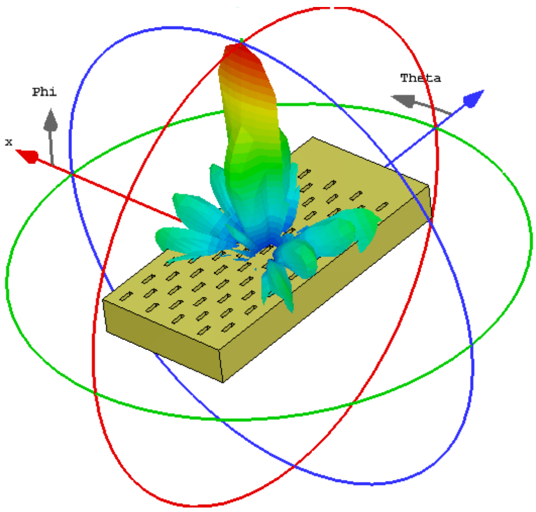

Figure 3. The proposed antenna array modeled in CST with the simulated 3D radiation pattern.

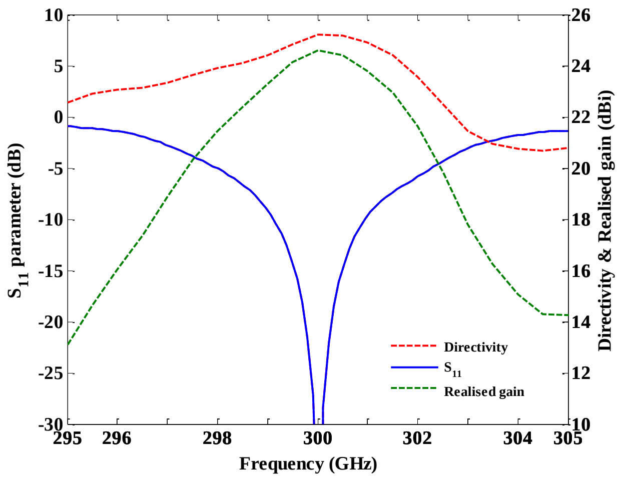

Figure 4. Variation of the simulated realised gain, directivity, and S_{11} of the antenna array.

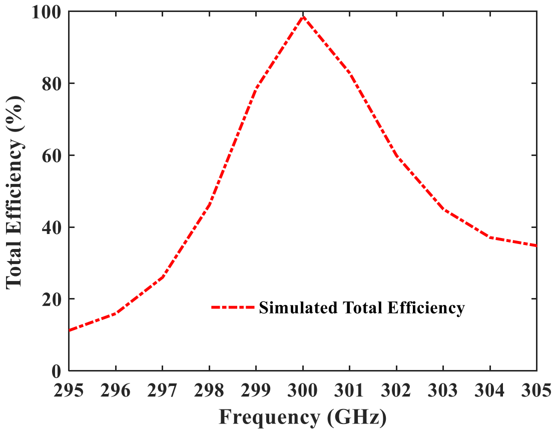

Figure 5. Variation of the simulated total efficiency of the antenna array.

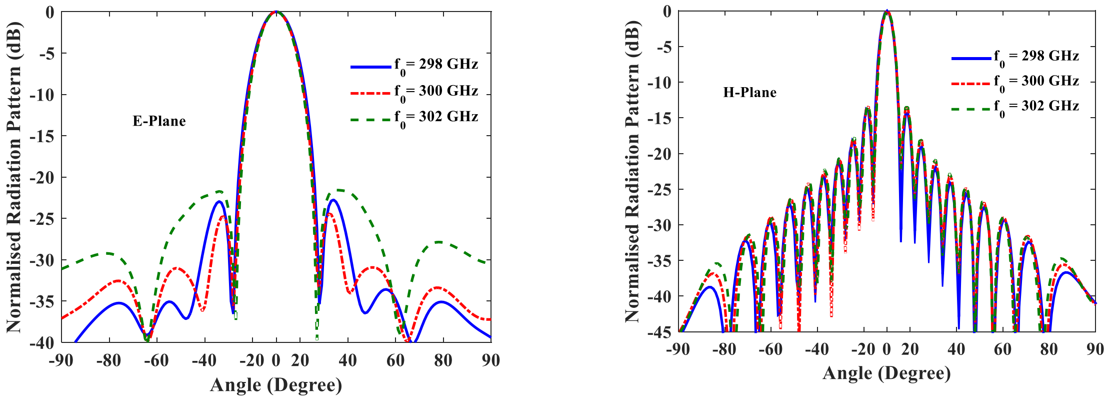

(**a**) (**b**)

Figure 6. The Simulated radiation patterns of the proposed antenna array at 298, 300, and 302 GHz respectively. (a) E-plane. (b) H-plane.

Table 2. Electrical performances of the proposed THz 8×8 planar array slotted waveguide antenna.

Parameters	Frequency (GHz)	Directivity (dBi)	Realised gain (dBi)	FBW (%)	3 dB Beam width (°)	Side lobe Level (dB)
Magnitude	300	25.2	24.6	1	E-plane = 13.5 H-plane = 5.1	E-plane = -24.4 H-plane = -13.4

3. Fabrication and Measurement

The antenna presented here was fabricated using the micromachining SU-8 lithography technique as discussed in [11, 13, 24, 32, 42]. This technique has been chosen due to providing high aspect ratio to form the rectangular waveguide structure and excellent side wall quality [43]. The antenna was configured to be built out of five SU-8 layers with a thickness of 0.288 mm. Only one mask is needed to define all the five SU-8 layers as shown in Fig. 7. Two brass-plates have been designed and utilized to clamp the five layers together and strengthen the device as illustrated in Fig. 8. The designed brass-plates have small influence on the S_{11} and the realised gain variation versus frequencies as can be noticed in Fig. 9.

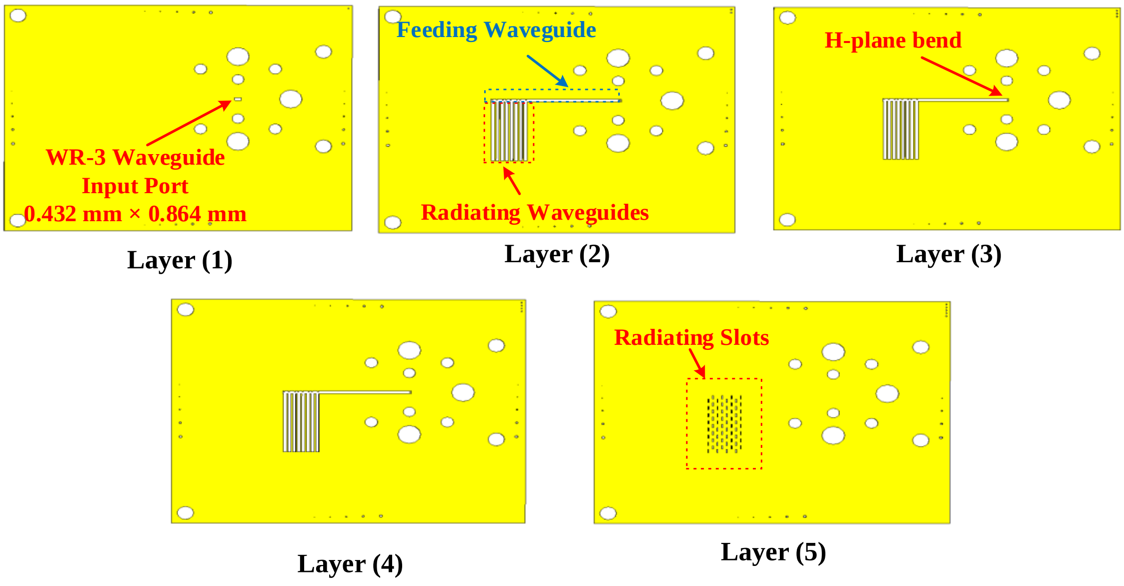

Figure 7. The top view of the five SU-8 equal-thickness layers of the proposed antenna array.

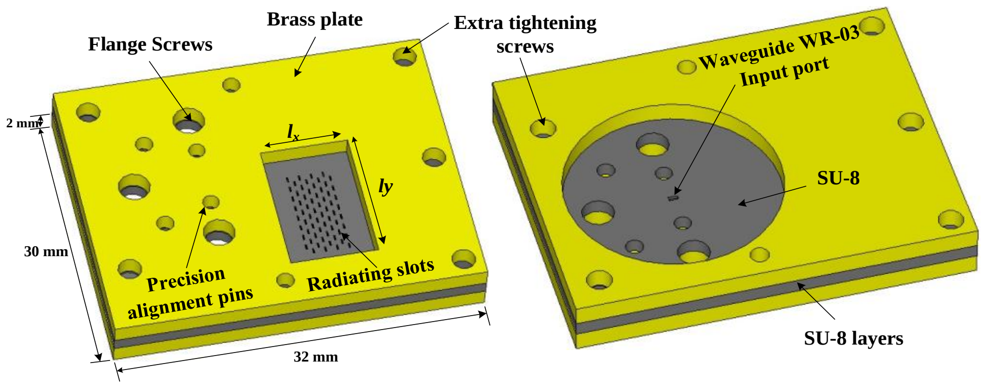

Figure 8. 3D view of the proposed 8×8 slotted waveguide antenna with the brass plates and the required holes labeled for alignment with the waveguide flange WR-03.

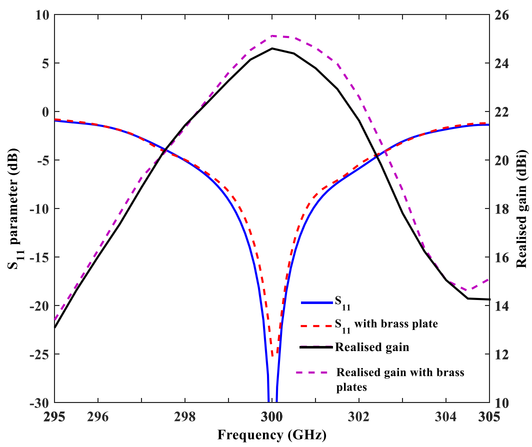

Figure 9. Effect of the brass-plates on the S_{11} and realised gain of the proposed antenna.

The SU-8 layer is an ultraviolet sensitive photoresist insulator, which is able to build 3D structure. In the design of a circuit like slotted waveguide antenna, it usually needs to be coated by a conductor. It has been investigated in [12] that the losses in a rectangular waveguide based on an SU-8 sliver coated are very comparable with a solid metal. In this work, five silver coated SU-8 layers is utilized in the design of the antenna array. It should be mentioned that the thickness of the SU-8 layer was originally designed to be 0.432 mm [11]. However, in this work, the thickness has been reduced to 0.288 mm in order to have a better sliver coating of the narrow side walls of the waveguides, slots, and the matching ridges. The fabrication process is comparatively simple, which can be performed following the four steps, as discussed below.

First, the thickness of the SU-8 was controlled by the amount of the resist weight. Here, 3.5 gram of SU-8-50 was used for each of a 0.288 mm layer thickness. The liquid SU-8 was span coated on a four inches silicon wafer. Then, the edge bead was removed directly. Second, two steps were used for the soft bake. In the first step, the bake was performed for 20 minutes at 65^0C. In the second step, the bake time was raised to 90 minutes at 95^0C. Third, the wafer was placed in a mask aligner (Canon PLA501) to expose a 365 nm ultra violet for 2 minutes interval. To eliminate the ultraviolet radiation, the PL360 filter was used. Moreover, to make a strong crosslink but with fewer stress, the post exposure bake was started for 2 minutes at 65^0C and then 30 minutes at 95^0C. Later, the wafer was left to cool down gradually to room temperature. The Ethylene Carbonate (EC) solvent was used to develop the SU-8 layers and make them more robust. Hard bake was performed eventually for 15 minutes at 150^0C. 10 % of the Potassium hydroxide (KOH) solution was used to release the SU-8 layers from the wafer. Finally, the released SU-8 layers were placed in the Cressington 308R evaporator in order to evaporate a 0.2 micron-thickness sliver and coat the side-walls of the waveguides and slots. To achieve homogenous coating, the SU-8 layers were tilted in an angle that the sliver evaporation was able to reach and cover the narrow side walls of the waveguides and the slots. It is important to mention here that the skin depth for a block of silver with conductivity of (6.3×10^7 S/m) is 291 nm at 300 GHz, which is much smaller than 2 microns. This confirms that the 2 microns silver coating does not introduce significant losses to the proposed antenna array. The five sliver coated SU-8 layers were assembled together with the brass-plates in a very precise manner in order to form the final device as shown in Fig. 10. The precision alignment pins were used to accurately align the device with the waveguide flange WR-03 and facilitate the measurement.

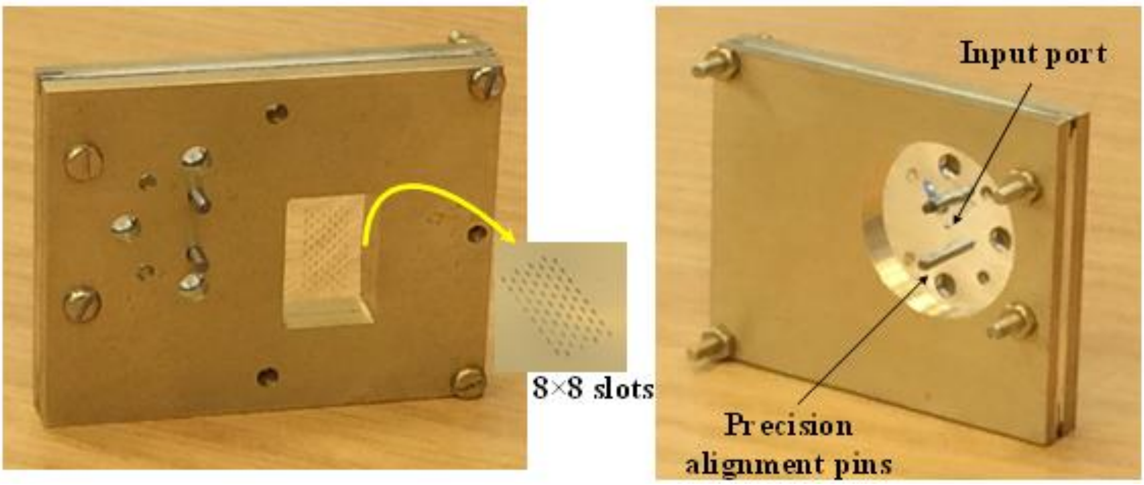

(**a**) (**b**)

Figure 10. Photograph of the fabricated planar array 8×8 slotted waveguide antenna based on the micromachined SU-8 technology. (a) Radiating side. (b) Back side.

The S_{11} parameter was measured in free space using the Agilent N5250-A Vector Network analyzer (VNA) at the University of Birmingham. Before connecting the antenna with the WR-03 extended port, one-port calibration (short-open-load aperture) was carried out. The measurement of the S_{11} was repeated for four times at the frequencies 220-325 GHz as presented in Fig. 11. It is seen that all the four responses are similar to each other, with some minor differences in the poles fluctuation magnitude. This goes back to the tightness of the screws used during the measurement each time to connect the antenna with the WR-03 extended port, and the insignificant misalignments which may have occurred.

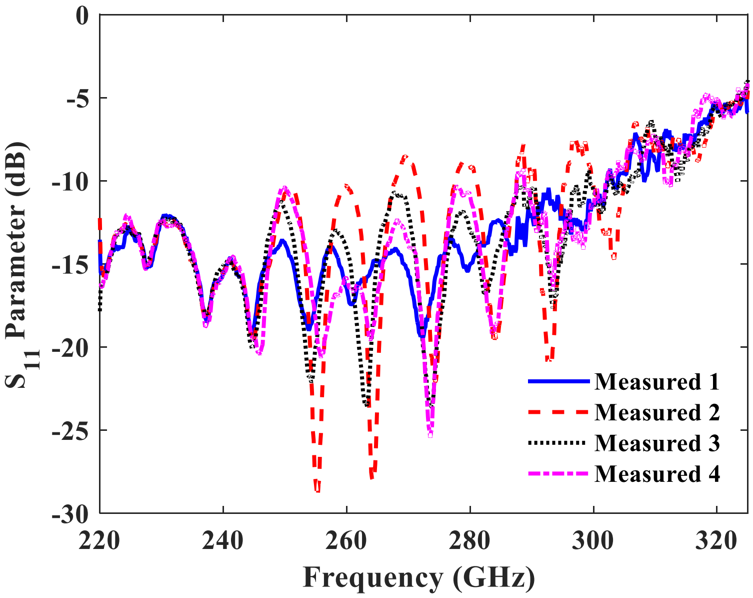

Figure 11. Measuring four times of S_{11} of the planar array 8×8 slotted waveguide antenna for validation of the measurement process.

On the other hand, there are some obvious differences depicted between the simulated and measured S_{11} responses. To find the reason, a closer attention was paid to the SU-8 layers using a digital microscope. Then, we have found that the top SU-8 layer has delaminated, as can be noticed from the top view of the actual device shown in Fig. 12. Therefore, the design is modified and re-modeled in the light of the delamination as shown in Fig. 13 in order to realize the delamination influence on the S_{11}response. It should be mentioned that the delamination has created a gap (g) between the top layer and the rest of the design. the g value is very small from both sides of the top SU-8 layer. However, it starts increasing until it reaches to its maximum value (g_m) (g_m~0.1 mm) at almost at the centre of the top SU-8 layer. This has been validated using the digital microscope. After taking many points into account and trying to make sure the re-modeled design looks like the same as the fabricated one, the antenna is then re-simulated. The re-simulated S_{11} response is compared with the measured in Fig. 14, and they are now comparable to each other. There are still some inconsistency between the re-simulated S_{11} response and the measured one. This could be due to the delamination manner, which is not exactly homogenous through the entire top SU-8 layer, while during the re-modeling in the CST we assume that it is homogenous.

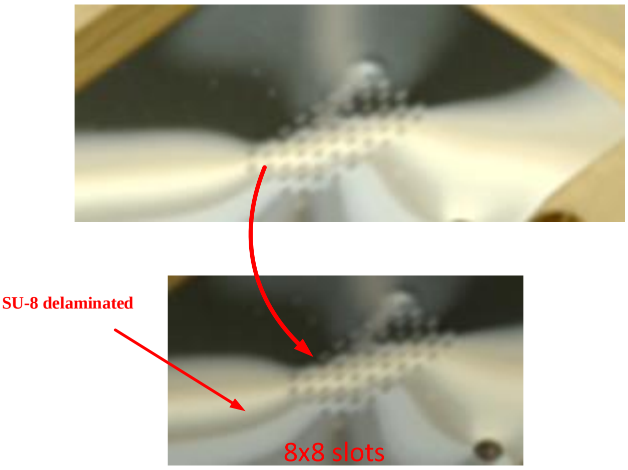

Fig. 12. Visualization of the delaminated SU-8 layer of the planar array 8×8 slotted waveguide antenna.

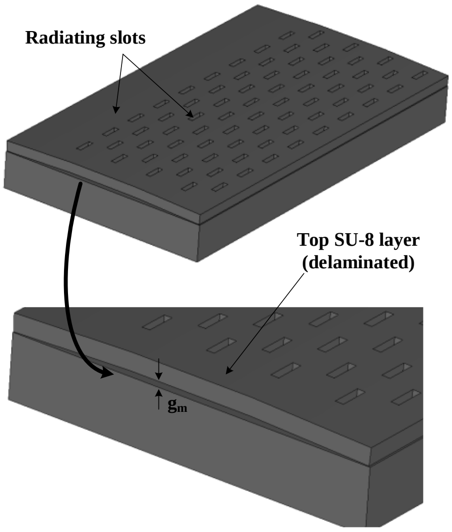

Fig. 13. CST model of the antenna design including the top SU-8 delaminated.

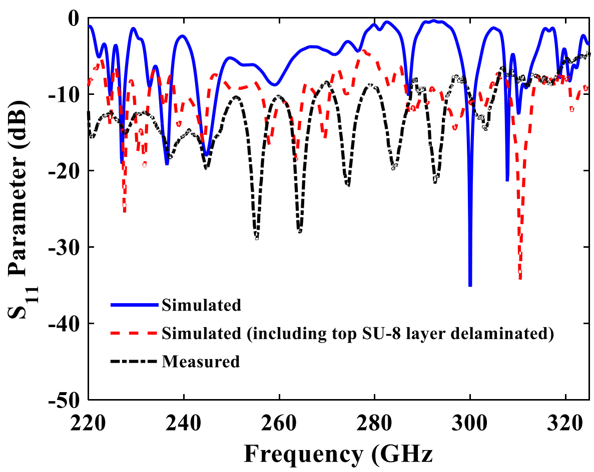

Fig. 14. Measured S_{11} of the planar array 8×8 slotted waveguide antenna compared with the simulated including the delamination.

Due to the lack of facilities, the radiation pattern was not measured. However, in order to validate the simulated radiation pattern, a comparison was made with the measured radiation pattern of an 8×8 antenna array waveguide based presented in [44]. It has been concluded that there are very close agreement between the simulated and measured patterns.

4. Conclusions

A micromachined 8×8 slotted waveguide antenna array has been demonstrated at lower THz frequencies. The antenna design was configured to be adapted to the micromachining SU-8 technology using five silver coated SU-8 layers. All the five layers were made out of a single SU-8 wafer. Two brass plates were designed and utilised to ensure the contact between the layers. The impact of the brasses on the antenna radiation performance is negligible. An H-plane bend has been embedded to the design to facilitate the interconnection with the VNA test port. Alignment pins were defined in all the SU-8 layers in order to avoid misalignment. The fabrication of the antenna was made. It was found that the top SU-8 layers were delaminated upwards. To maintain a reliable comparison between measured and simulated results, the antenna is re-modeled in the CST including the modifications occurred due to the delamination. After this, the measured S_{11} is very comparable with the simulation. The proposed antenna has planar structure which could simply be integrated with other components when employing in some indoor wireless systems and sensors. The proposed fabrication process for the antennas operating at THz frequencies is simple and cost-effective.

Funding: This work was supported partially by the U.K. Engineering and Physical Science Research Council under Contract EP/H029656/1.

Conflicts of Interest: The authors declare no conflict of interest.

Availability of data and material: Not applicable

Code availability: Not applicable

Author Contribution: Conceptualization: Rashad H. Mahmud, Michael J. Lancaster, and Xiaobang Shang; Methodology: Rashad H. Mahmud, Michael J. Lancaster, and Xiaobang Shang; Formal analysis and investigation: Yi Wang, Halgurd N. Awl, Idris H. Salih, and Talal Skaik; Writing - original draft preparation: Rashad H. Mahmud; Writing - review and editing: Michael J. Lancaster, Yi Wang, Talal Skaik, Idris H. Salih; Supervision: Michael J. Lancaster.

Ethics approval: Not applicable

Consent to Participate: Informed consent was obtained from all authors.

Consent for publication: The authors confirm that there is informed consent to the publication of the data contained in the article.

References

[1] H. Lu, X. Lv, K. Zhou, and Y. Liu, "Experimental realisation of micromachined terahertz waveguide-fed antipodal tapered slot antenna," *Electronics letters,* vol. 50, pp. 615-617, 2014.

[2] C. Debus and P. H. Bolívar, "Terahertz biosensors based on double split ring arrays," in *Metamaterials III*, 2008, p. 69870U.

[3] N. Llombart, K. B. Cooper, R. J. Dengler, T. Bryllert, and P. H. Siegel, "Confocal ellipsoidal reflector system for a mechanically scanned active terahertz imager," *IEEE Transactions on Antennas and Propagation,* vol. 58, pp. 1834-1841, 2010.

[4] P. H. Siegel, "Terahertz technology in biology and medicine," *IEEE transactions on microwave theory and techniques,* vol. 52, pp. 2438-2447, 2004.

[5] P. H. Siegel, "THz instruments for space," *IEEE Transactions on Antennas and Propagation,* vol. 55, pp. 2957-2965, 2007.

[6] S. Galoda and G. Singh, "Fighting terrorism with terahertz," *Ieee Potentials,* vol. 26, pp. 24-29, 2007.

[7] Y.-S. Lee, *Principles of terahertz science and technology* vol. 170: Springer Science & Business Media, 2009.

[8] K. R. Jha and G. Singh, *Terahertz planar antennas for next generation communication*: Springer, 2014.

[9] P. H. Siegel, "Terahertz technology," *IEEE Transactions on microwave theory and techniques,* vol. 50, pp. 910-928, 2002.

[10] D. F. Filipovic, S. S. Gearhart, and G. M. Rebeiz, "Double-slot antennas on extended hemispherical and elliptical silicon dielectric lenses," *IEEE Transactions on microwave theory and techniques,* vol. 41, pp. 1738-1749, 1993.

[11] Y. Wang, M. Ke, M. J. Lancaster, and J. Chen, "Micromachined 300-GHz SU-8-based slotted waveguide antenna," *IEEE Antennas and Wireless Propagation Letters,* vol. 10, pp. 573-576, 2011.

[12] X. Shang, M. Ke, Y. Wang, and M. J. Lancaster, "WR-3 band waveguides and filters fabricated using SU8 photoresist micromachining technology," *IEEE Transactions on Terahertz Science and Technology,* vol. 2, pp. 629-637, 2012.

[13] X. Shang, Y. Tian, M. J. Lancaster, and S. Singh, "A SU8 micromachined WR-1.5 band waveguide filter," *IEEE microwave and wireless components letters,* vol. 23, pp. 300-302, 2013.

[14] Y. Wang, X. Shang, and M. J. Lancaster, "Micromachined 3D millimeter-wave and terahertz devices," in *2015 IEEE MTT-S International Microwave Workshop Series on Advanced Materials and Processes for RF and THz Applications (IMWS-AMP)*, 2015, pp. 1-3.

[15] R. Mahmud, T. He, M. Lancaster, Y. Wang, and X. Shang, "Micromachined travelling wave slotted waveguide antenna array for beam-scanning applications," in *10th Loughborough Antennas and Propagation Conference, LAPC*, 2014.

[16] J. Zhang, Q. Hong, J. Zou, Y. He, X. Yuan, Z. Zhu*, et al.*, "Fano-Resonance in Hybrid Metal-Graphene Metamaterial and Its Application as Mid-Infrared Plasmonic Sensor," *Micromachines,* vol. 11, p. 268, 2020.

[17] P. Granitzer, R. Boukherroub, D. J. Lockwood, and H. Masuda, "Pits & Pores 6: Nanomaterials-in Memory of Yukio H. Ogata," 2015.

[18] G. J. Lee, H. M. Kim, and Y. M. Song, "Design and Fabrication of Microscale, Thin-Film Silicon Solid Immersion Lenses for Mid-Infrared Application," *Micromachines*, vol. 11, p. 250, 2020.

[19] S. Sekretarov and D. M. Vavriv, "A wideband slotted waveguide antenna array for SAR systems," *Progress in Electromagnetics Research,* vol. 11, pp. 165-176, 2010.

[20] K. Sakakibara, J. Hirokawa, M. Ando, and N. Goto, "High-gain and high-efficiency single-layer slotted waveguide array for use in 22 GHz band," *Electronics Letters,* vol. 32, pp. 283-284, 1996.

[21] R. Gardelli, M. Albani, and F. Capolino, "Array thinning by using antennas in a Fabry–Perot cavity for gain enhancement," *IEEE Transactions on Antennas and Propagation,* vol. 54, pp. 1979-1990, 2006.

[22] C. Mateo-Segura, G. Goussetis, and A. P. Feresidis, "Sub-wavelength profile 2-D leaky-wave antennas with two periodic layers," *IEEE Transactions on Antennas and Propagation,* vol. 59, pp. 416-424, 2010.

[23] S. A. Muhammad, R. Sauleau, and H. Legay, "Small-size shielded metallic stacked Fabry–Perot cavity antennas with large bandwidth for space applications," *IEEE Transactions on antennas and propagation,* vol. 60, pp. 792-802, 2011.

[24] K. Konstantinidis, A. P. Feresidis, Y. Tian, X. Shang, and M. J. Lancaster, "Micromachined terahertz Fabry–Perot cavity highly directive antennas," *IET Microwaves, Antennas & Propagation,* vol. 9, pp. 1436-1443, 2015.

[25] R. H. Mahmud and M. J. Lancaster, "High-gain and wide-bandwidth filtering planar antenna array-based solely on resonators," *IEEE Transactions on Antennas and Propagation*, vol. 65, pp. 2367-2375, 2017.

[26] H. Guan-Long, Z. Shi-Gang, C. Tan-Huat, and Y. Tat-Soon, "Broadband and high gain waveguide-fed slot antenna array in the Ku-band," *IET Microwaves, Antennas & Propagation*, vol. 8, pp. 1041-1046, 2014.

[27] M. Ando, J. Hirokawa, T. Yamamoto, A. Akiyama, Y. Kimura, and N. Goto, "Novel single-layer waveguides for high-efficiency millimeter-wave arrays," *IEEE transactions on microwave theory and techniques*, vol. 46, pp. 792-799, 1998.

[28] Y. Kimura, Y. Miura, T. Shirosaki, T. Taniguchi, Y. Kazama, J. Hirokawa, *et al.*, "A low-cost and very compact wireless terminal integrated on the back of a waveguide planar array for 26 GHz band fixed wireless access (FWA) systems," *IEEE transactions on antennas and propagation*, vol. 53, pp. 2456-2463, 2005.

[29] J. Hirokawa, M. Zhang, and M. Ando, "94GHz fabrication of a slotted waveguide array antenna by diffusion bonding of laminated thin plates," in *SENSORS, 2009 IEEE*, 2009, pp. 907-911.

[30] J. Hirokawa, M. Ando, N. Goto, N. Takahashi, T. Ojima, and M. Uematsu, "A single-layer slotted leaky waveguide array antenna for mobile reception of direct broadcast from satellite," *IEEE transactions on vehicular technology*, vol. 44, pp. 749-755, 1995.

[31] M. Ando, "Planar waveguide arrays for millimeter wave systems," *IEICE transactions on communications*, vol. 93, pp. 2504-2513, 2010.

[32] R. H. Mahmud, "Synthesis of waveguide antenna arrays using the coupling matrix approach," University of Birmingham, 2016.

[33] R. C. Johnson and H. Jasik, "Antenna engineering handbook," *New York, McGraw-Hill Book Company, 1984, 1356 p. No individual items are abstracted in this volume.*, 1984.

[34] A. Stevenson, "Theory of slots in rectangular wave-guides," *Journal of Applied physics*, vol. 19, pp. 24-38, 1948.

[35] R. Stegen, "Slot radiators and arrays at X-band," *Transactions of the IRE Professional Group on Antennas and Propagation*, vol. 1, pp. 62-84, 1952.

[36] A. Oliner, "The impedance properties of narrow radiating slots in the broad face of rectangular waveguide: Part I--Theory," *IRE Transactions on Antennas and Propagation*, vol. 5, pp. 4-11, 1957.

[37] R. Elliott and L. Kurtz, "The design of small slot arrays," *IEEE Transactions on Antennas and Propagation*, vol. 26, pp. 214-219, 1978.

[38] C. MWS, "Computer Simulation Technology: Microwave Studio," *Computer Simulation Technology Std*, 2011.

[39] D. M. Pozar, *Microwave engineering*: John Wiley & Sons, 2009.

[40] C. A. Balanis, *Antenna theory: analysis and design*: John wiley & sons, 2016.

[41] Y. Wang and M. Lancaster, "A micromachined centre-fed slotted waveguide antenna for mm-wave applications," in *2012 IEEE MTT-S International Microwave Workshop Series on Millimeter Wave Wireless Technology and Applications*, 2012, pp. 1-3.

[42] Y. Wang, B. Yang, Y. Tian, R. S. Donnan, and M. J. Lancaster, "Micromachined thick mesh filters for millimeter-wave and terahertz applications," *IEEE Transactions on Terahertz Science and Technology,* vol. 4, pp. 247-253, 2014.

[43] J. D. Williams and W. Wang, "Study on the postbaking process and the effects on UV lithography of high aspect ratio SU-8 microstructures," *Journal of Micro/Nanolithography, MEMS, and MOEMS,* vol. 3, pp. 563-569, 2004.

[44] A. Vosoogh and P.-S. Kildal, "Corporate-fed planar 60-GHz slot array made of three unconnected metal layers using AMC pin surface for the gap waveguide," *IEEE Antennas and Wireless Propagation Letters,* vol. 15, pp. 1935-1938, 2015.